

Large- and Small-Scale Dynamics of Variable-Density Rayleigh-Taylor Instability-Induced Turbulent Mixing



Oleg Schilling and Andrew W. Cook

University of California, Lawrence Livermore National Laboratory
P.O. Box 808, L-22, Livermore, CA 94551
(925) 423-6879, schilling1@llnl.gov



Presented at the
8th International Workshop on the Physics of Compressible Turbulent Mixing
California Institute of Technology, Pasadena, CA
9-14 December 2001

This work was performed under the auspices of the U.S. Department of Energy by the
University of California, Lawrence Livermore National Laboratory under Contract No. W-7405-Eng-48

Oleg Schilling
IWPCTM-12/01 1

The dynamical effects of 'small' (unresolved) scales on 'large' (resolved) scales cannot be neglected in a turbulent mixing layer



- The dynamical effect of small scales on large scales is a bi-directional, competing process
 - Energy transferred **up** and **down** scale through 'backscatter' and a cascade, respectively, over a wide range of eddies
 - As Re increases, contribution from the small scales increases
- *Rate of scalar mixing* is proportional to dissipation rate of the squared scalar ($\langle \cdot \rangle$ is an average and D is the scalar diffusion coefficient)

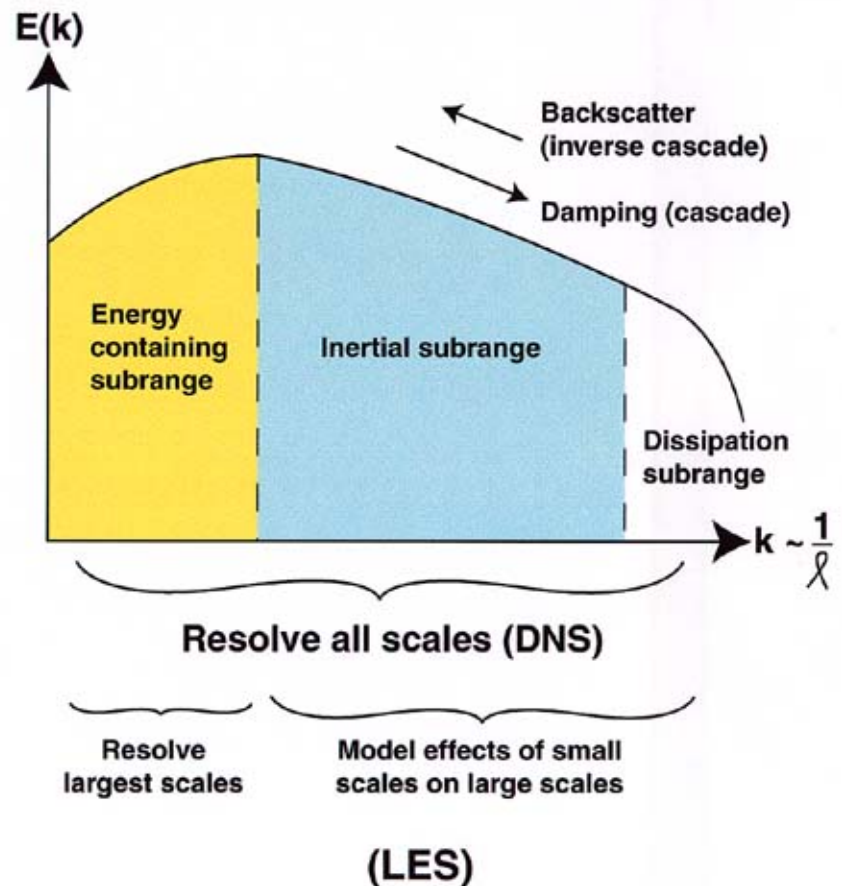
$$\langle \epsilon_\phi \rangle \equiv -\frac{\partial}{\partial t} \left\langle \frac{\phi^2}{2} \right\rangle = D \langle \phi \nabla^2 \phi \rangle$$

- *Contribution to this quantity is dominated by the small scales*, where gradients are large
- Turbulent quantities (e.g., the kinetic energy) are contributed by all scales, not only by large-scale, integral quantities
- Simulation of Rayleigh-Taylor mixing requires capability to simulate smaller scales as well as the largest scales

Schematic of direct numerical simulation (DNS) and large-eddy simulation (LES) for turbulent mixing



- Turbulence enhances mass, momentum, energy transport
 - Coherent bubble/spike structures associated with energy containing subrange
- Energy *transferred* among eddies at all scales
 - Inertial subrange 'mediates' between largest and smallest scales
- Molecular (atomic) mixing associated with dissipation subrange, in which structures are too small to be resolved



The approaches used thus far to simulate Rayleigh-Taylor mixing have important physical and computational limitations



- Monotone integrated LES (MILES)
 - Implicit numerical dissipation (finite-volume simulations of the non-dissipative equations)
 - **Advantage**: modest computational requirements
 - **Disadvantage**: small-scale structures and statistics not estimated well, while large-scale structures and lowest-order integral properties are
- DNS
 - Physical dissipation (spectral and finite-difference simulations of the dissipative equations)
 - **Advantage**: all structures and statistics estimated well
 - **Disadvantage**: very high computational and data storage/processing requirements

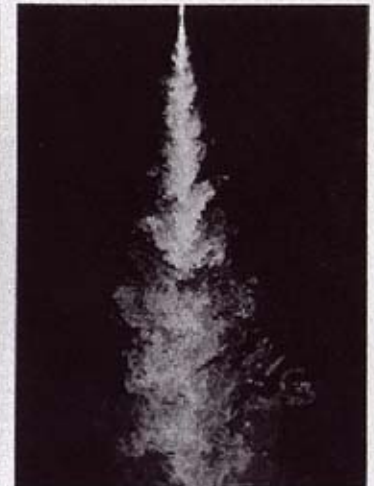
High-resolution DNS is too computationally expensive to simulate Rayleigh-Taylor mixing: an LES capability is needed



- DNS is too expensive to simulate a mixing layer that exceeds the *mixing transition Reynolds number* $Re \sim 10^4$
 - Issue is more acute for miscible, **reacting** flows in which all scales are below any possible grid resolution
- Therefore, development of a true LES capability to predict mean hydrodynamic fields and lowest-order transport and mixing statistics is essential

$Re \sim 2.5 \times 10^3$

$Re \sim 1 \times 10^4$



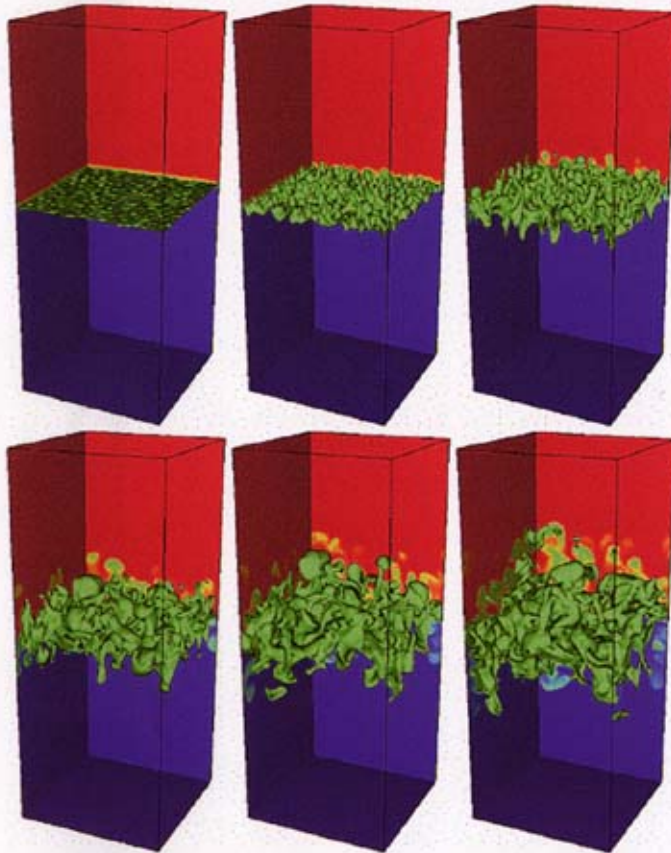
Liquid-jet concentration in a round turbulent jet (Dimotakis 1983)

To develop an LES capability, an examination of interaction between unresolved and resolved scales in Rayleigh-Taylor mixing layers is needed



- Study transfer (exchange) of $\rho^2/2$ and $v^2/2$ among different wavenumber regions (corresponding to spatial scales or eddies)
 - ρ and v_i fields obtained from high-resolution DNS data
 - An artificial cutoff scale is used to partition scales into computationally **resolved** and **unresolved** scales
- Fourier space representation determines magnitude and other properties of transfer process as a function of scale k and height in the domain
 - **Wavelet transforms** can also be used to add information as a *function of position*
- Data obtained from this study will be used to develop and assess subgrid-scale and backscatter models for LES
 - Work will improve the classical Smagorinsky eddy viscosity and scale-similarity subgrid-scale models

A high-resolution ($512^2 \times 2040$) DNS was performed for miscible, variable-density, Rayleigh-Taylor unstable fluids with $At = 1/2$



Density isosurface at times 1, 2, 3, 4, 5, 6
red: $\rho = 3$; green: $\rho = 2$; blue: $\rho = 1$

- Spectral/8th-order compact finite-difference method with 3rd-order, Adams-Bashforth time-evolution
- Small-scale initial perturbations on fluid interface
- Turbulence attains late-time Reynolds number based on mixing layer width

$$Re_h(t) = \frac{(\rho_1 + \rho_2)}{2\mu} h(t) \frac{dh(t)}{dt} \approx 5.5 \times 10^3$$

Similarly, the analysis of kinetic energy transfer dynamics begins with a 2-dimensional Fourier transform of the momentum equation



- Applying the Fourier transform to the momentum equation in homogeneous directions gives ($V = 1/\rho$ is the specific volume)

$$\frac{\partial v_i(\mathbf{k}_\perp, z, t)}{\partial t} \equiv \underbrace{F_i(\mathbf{k}_\perp, z, t)}_{\text{forcing term}} + \underbrace{N_i(\mathbf{k}_\perp, z, t)}_{\text{advection term}} + \underbrace{D_i(\mathbf{k}_\perp, z, t)}_{\text{dissipation terms}}$$

$$= -g(t) \delta_{i3}$$

$$-\iint V(\mathbf{p}_\perp, z, t) \left(i q_\perp^i + \delta^{i3} \frac{\partial}{\partial z} \right) p(\mathbf{q}_\perp, z, t) \delta^2(\mathbf{k}_\perp - \mathbf{p}_\perp - \mathbf{q}_\perp) d^2 p_\perp d^2 q_\perp$$

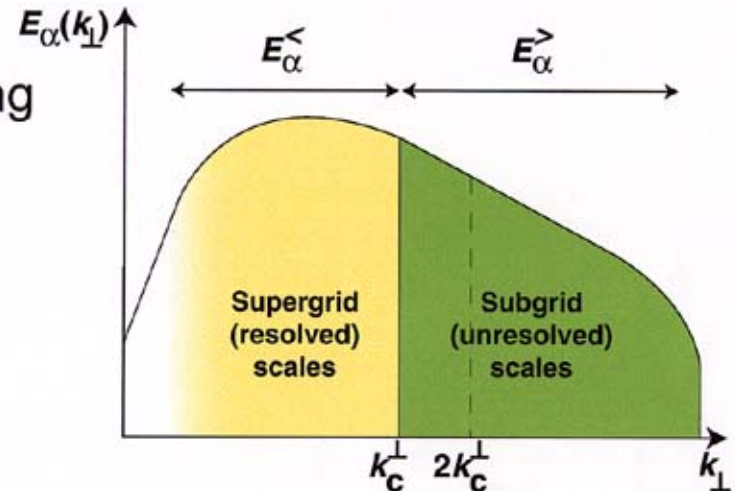
$$-\iint v_j(\mathbf{p}_\perp, z, t) \left(i q_\perp^j + \delta^{j3} \frac{\partial}{\partial z} \right) v_i(\mathbf{q}_\perp, z, t) \delta^2(\mathbf{k}_\perp - \mathbf{p}_\perp - \mathbf{q}_\perp) d^2 p_\perp d^2 q_\perp$$

$$-v \left(k_\perp^2 - \frac{\partial^2}{\partial z^2} \right) v_i(\mathbf{k}_\perp, z, t) - \frac{4}{3} v k_\perp^i k_\perp^j v_j(\mathbf{k}_\perp, z, t)$$

For a given k_{\perp} , N_{ρ} and N_i describe the integrated nonlinear interactions of *all other scales* with k_{\perp}



- Decompose nonlinear terms into partial sum N_{ρ}^A and N_i^A corresponding to different disjoint regions $A \ni k_{\perp}$
 - Each term represents nonlinear interactions contributed by any 2 such regions
- Define regions



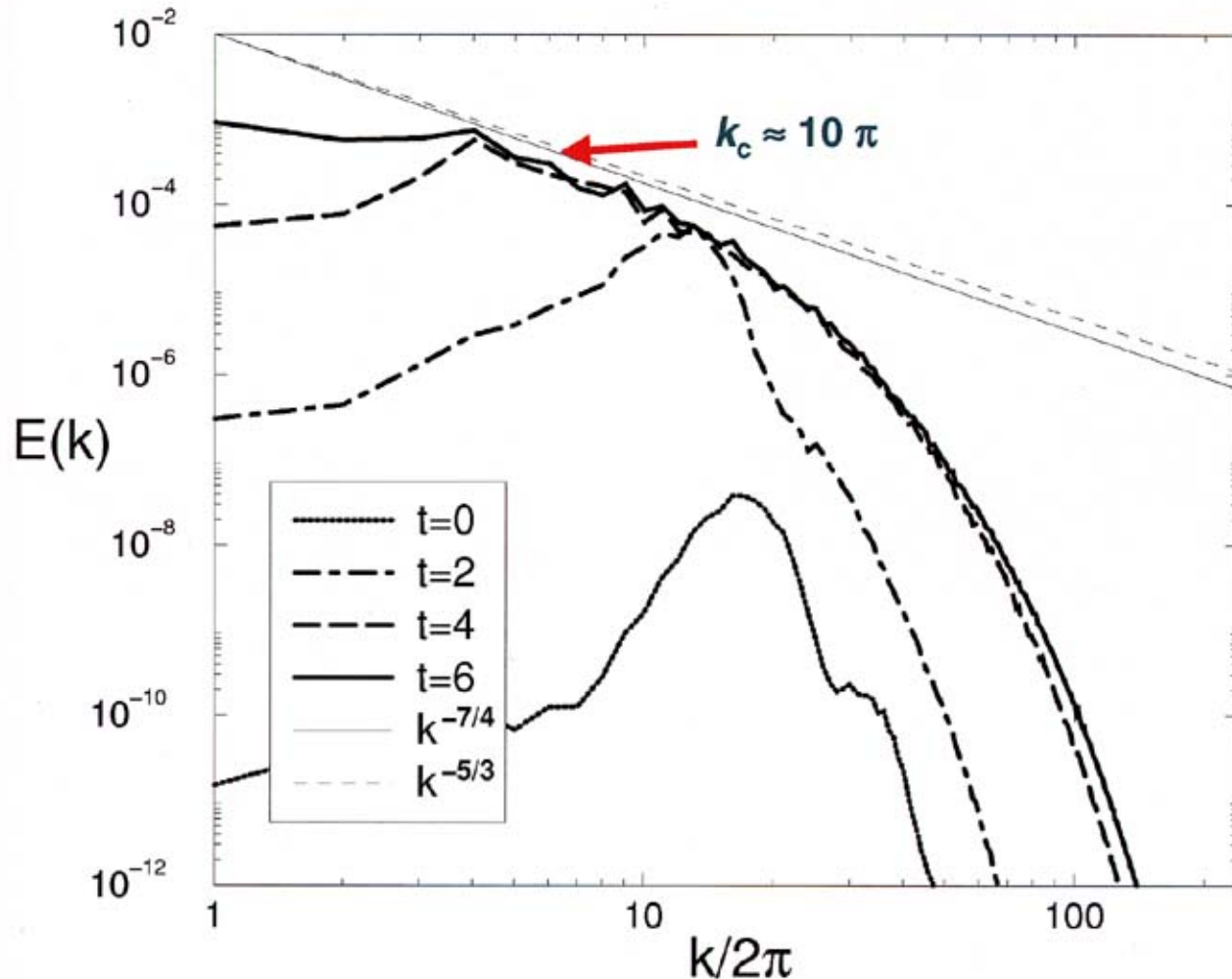
$$k_0^{\perp} = 0 < k_1^{\perp} = k_c^{\perp} < k_2^{\perp} = 2k_c^{\perp} < k_3^{\perp} = k_{max}^{\perp}$$

where k_c^{\perp} and k_{max}^{\perp} are cutoff and maximum wavenumbers

- Partial nonlinear terms computed by truncating v_i and ρ to region A ,

$$\phi_{\alpha}^A(\mathbf{k}_{\perp}, z, t) \equiv \begin{cases} \phi_{\alpha}(\mathbf{k}_{\perp}, z, t) & \mathbf{k}_{\perp} \in A \\ 0 & \text{otherwise} \end{cases}$$

The kinetic energy spectrum at the midplane ($z = 0$) evolves to a state with a very short inertial subrange



Previous decomposition of nonlinear terms can be used to derive expressions for supergrid and subgrid nonlinear terms



- The nonlinear term describing interactions of modes $k_{\perp} \in K$ with modes in regions P and Q can be expressed as a sum

$$N_{\alpha}(\mathbf{k}_{\perp}, z, t) = \sum_{K=1}^3 \sum_{P=1}^3 \sum_{Q \geq P=1}^3 N_{\alpha}^{K P Q}(\mathbf{k}_{\perp}, z, t)$$

- Supergrid** (resolved) nonlinear terms corresponding to modes $k_{\perp} < k_c^{\perp}$ and to modes $k_{\perp} < k_2^{\perp} = 2 k_c^{\perp}$:

$$N_{\alpha}^{<}(\mathbf{k}_{\perp} | \mathbf{k}_{\perp}^c, z, t) = N_{\alpha}^{111}$$

$$N_{\alpha}^{<}(\mathbf{k}_{\perp} | 2\mathbf{k}_{\perp}^c, z, t) = N_{\alpha}^{111} + N_{\alpha}^{121} + N_{\alpha}^{221} + N_{\alpha}^{112} + N_{\alpha}^{122} + N_{\alpha}^{222}$$

- Subgrid** (unresolved) nonlinear terms corresponding to modes $k_{\perp} > k_c^{\perp}$ and to modes $k_c^{\perp} > k_2^{\perp} = 2 k_c^{\perp}$:

$$N_{\alpha}^{>}(\mathbf{k}_{\perp} | \mathbf{k}_{\perp}^c, z, t) = N_{\alpha}^{121} + N_{\alpha}^{131} + N_{\alpha}^{221} + N_{\alpha}^{231} + N_{\alpha}^{331}$$

$$N_{\alpha}^{>}(\mathbf{k}_{\perp} | 2\mathbf{k}_{\perp}^c, z, t) = N_{\alpha}^{131} + N_{\alpha}^{231} + N_{\alpha}^{331} + N_{\alpha}^{132} + N_{\alpha}^{232} + N_{\alpha}^{332}$$

The supergrid and subgrid energy density evolution equations can be formed in terms of the nonlinear terms



- Partial transfer spectra describe rate of $\rho^2/2$ and $v^2/2$ change in modes $\mathbf{k}_\perp \in K$ due to nonlinear interactions between modes $\mathbf{p}_\perp \in P$ and $\mathbf{q}_\perp \in Q$:

$$T_\alpha^{K PQ}(\mathbf{k}_\perp, z, t) = \text{Re} \left[\phi_\alpha(\mathbf{k}_\perp, z, t)^* N_\alpha^{K PQ}(\mathbf{k}_\perp, z, t) \right]$$

- Introducing large-scale density and velocity truncated at $k_2^\perp = 2 k_c^\perp$,

$$\rho^< = \rho^1 + \rho^2 \quad , \quad v_i^< = v_i^1 + v_i^2$$

the supergrid (resolved) density squared and kinetic energy are

$$E_\rho^<(\mathbf{x}, t) = \frac{\rho^<(\mathbf{x}, t)^2}{2} \quad , \quad E^<(\mathbf{x}, t) = \frac{v^<(\mathbf{x}, t)^2}{2}$$

- The equations for these quantities contain the supergrid and subgrid transfers

The subgrid-scale energy transfer spectra $T_\alpha(k_\perp|k_c^\perp; z, t)$ provide information on *magnitude* and *direction* of the energy transfer



- Computation of subgrid-scale energy transfers requires summation over all k_\perp in a spherical shell centered around k_c^\perp :

$$T_\alpha^{>}(k_\perp|k_c^\perp; z, t) = \sum_{k_\perp - \frac{\Delta k_\perp}{2} < |k_\perp| < k_\perp + \frac{\Delta k_\perp}{2}} T_\alpha^{>PQ}(k_\perp|k_c^\perp; z, t)$$

where P and Q are spherical wavenumber bands centered around p_\perp and q_\perp

- Computation involves interactions in which components of the sum can be either positive or negative

- Positive component (forward energy cascade):

$$T_\alpha^{(+)>}(k_\perp|k_c^\perp; z, t) \equiv \frac{T_\alpha^{>}(k_\perp|k_c^\perp; z, t) + |T_\alpha^{>}(k_\perp|k_c^\perp; z, t)|}{2}$$

- Negative component (backward energy cascade):

$$T_\alpha^{(-)>}(k_\perp|k_c^\perp; z, t) \equiv \frac{T_\alpha^{>}(k_\perp|k_c^\perp; z, t) - |T_\alpha^{>}(k_\perp|k_c^\perp; z, t)|}{2}$$

Net eddy viscosities $\nu_\alpha^n(k_\perp | k_\perp^c; z, t)$ can be defined for $k_\perp < k_\perp^c$ in terms of eddy and backscatter viscosities



- Net eddy viscosities:

$$\nu_\alpha^n(k_\perp | k_\perp^c; z, t) \equiv -\frac{T_\alpha^>(k_\perp | k_\perp^c; z, t)}{2k_\perp^2 E_\alpha^<(k_\perp, z, t)}$$

- Eddy viscosities: (representing energy removal by small scales)

$$\nu_\alpha(k_\perp | k_\perp^c; z, t) \equiv -\frac{T_\alpha^{(+)>}(k_\perp | k_\perp^c; z, t)}{2k_\perp^2 E_\alpha^<(k_\perp, z, t)}$$

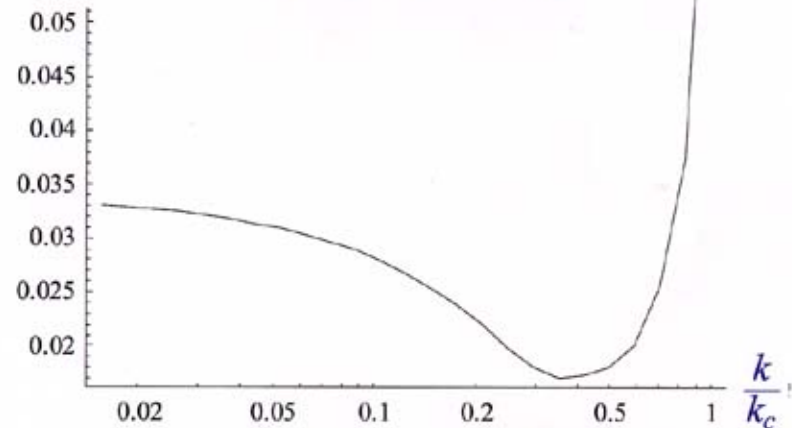
- Backscatter viscosities: (representing energy transfer from small to larger scales)

$$\nu_\alpha^b(k_\perp | k_\perp^c; z, t) \equiv \frac{T_\alpha^{(-)>}(k_\perp | k_\perp^c; z, t)}{2k_\perp^2 E_\alpha^<(k_\perp, z, t)}$$

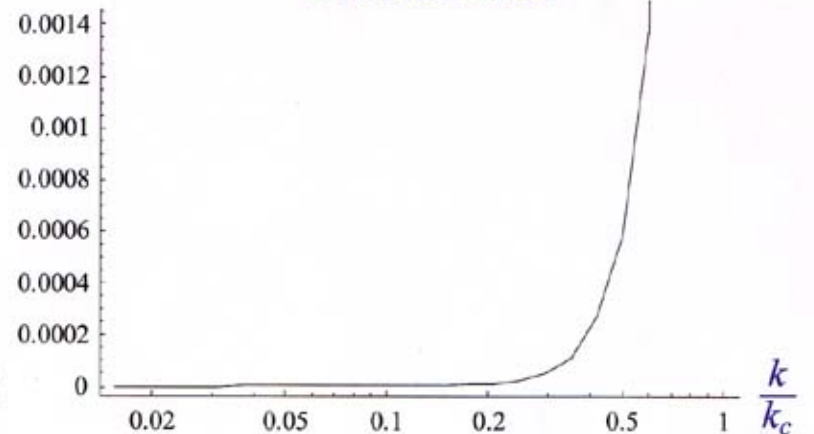
- Thus, net viscosities are

$$\nu_\alpha^n(k_\perp | k_\perp^c; z, t) = \nu_\alpha(k_\perp | k_\perp^c; z, t) - \nu_\alpha^b(k_\perp | k_\perp^c; z, t)$$

Eddy viscosity



Backscatter



Given the eddy and backscatter viscosities, a subgrid-scale model can be defined



- Large-eddy equations have the form (only the Navier-Stokes equation is shown)

$$\frac{\partial}{\partial t} (\rho^< v_i^<) + \frac{\partial}{\partial x_j} (\rho^< v_i^< v_j^< + p \delta_{ij} - \sigma_{ij}) - \rho^< g_i = - \frac{\partial \tau_{ij}}{\partial x_j}$$

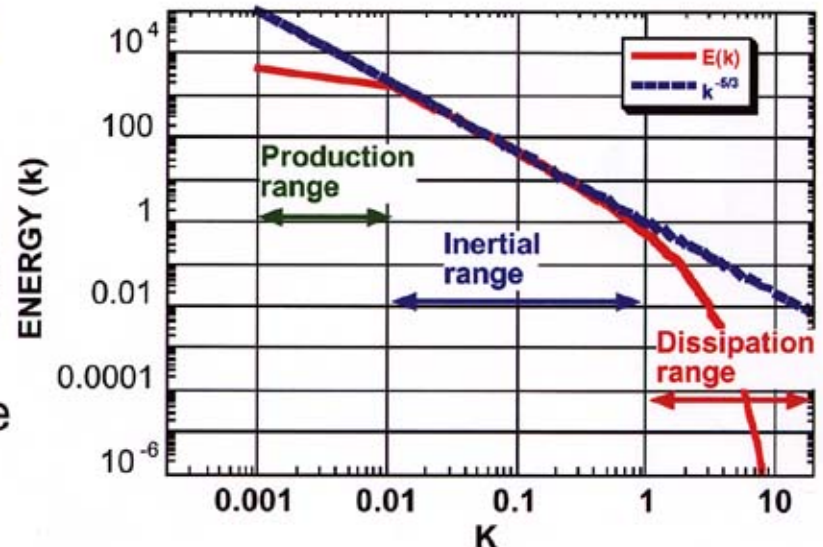
- Left side is computed explicitly
- Right side involves the Reynolds stress tensor τ_{ij}

– The Smagorinsky model is

$$\tau_{ij} = \frac{\delta_{ij}}{3} (v^<) ^2 - \nu_t \left(\frac{\partial v_i^<}{\partial x_j} + \frac{\partial v_j^<}{\partial x_i} \right)$$

- A similar parameterization may be reasonable for resolved density equation

Spectrum of turbulence



Turbulence dynamics of enstrophy (vorticity squared) transfer is particularly relevant to interfacial instability-induced turbulent mixing



- Dynamics of enstrophy $\rho \Omega = \rho \omega^2 / 2$ will also be examined (dissipation terms are not written)

$$\frac{\partial}{\partial t} (\rho \Omega) + \frac{\partial}{\partial x_j} (\rho \Omega v_j) = \underbrace{\epsilon_{ijk} \frac{\omega^i}{\rho} \frac{\partial \rho}{\partial x_j} \frac{\partial p}{\partial x_k}}_{\text{baroclinic production}} + \underbrace{\rho \omega_i S^{ij} \omega_j}_{\text{enstrophy stretching}} - \underbrace{2 \rho \Omega \frac{\partial v_j}{\partial x_j}}_{\text{dilatation}}$$

- Baroclinic production term is an instability source term, existing due to **misalignment of $\nabla \rho$ and ∇p**
- Stretching term is related to development of turbulence
- Dilatation term is small in a variable-density flow, but is important in a compressible (Richtmyer-Meshkov) flow
- Baroclinic production and stretching terms exist in 3D, but only the former exists in 2D
 - Nature of turbulent energy and enstrophy cascades is, therefore, very different in 2D and 3D

Conclusions and work in progress



- A subgrid-scale transfer analysis can be applied to Rayleigh-Taylor and Richtmyer-Meshkov mixing layers
 - Provides time- and scale-dependent measure of energy transfer process
 - Provides parameterizable eddy viscosities/backscatters for LES of Rayleigh-Taylor mixing at large Re
 - Also provides information for scale-similarity and more recent deconvolution subgrid-scale models
- Data processing at LLNL requires 256 IBM SP nodes (1,024 CPUs) and sufficient computer time
- Purpose of this research is to acquire physical insight into coupling of the large and small scales, in order to develop and assess subgrid-scale models for LES